# THEORETICAL AND NUMERICAL APPROACH OF THE BOND BEHAVIOR IN BEAM TESTS USING SELF-COMPACTING AND ORDINARY CONCRETE WITH THE SAME COMPRESSIVE STRENGTH

ABORDAGEM TEÓRICA E NUMÉRICA DO COMPORTAMENTO DE ADERÊNCIA EM VIGAS UTILIZANDO CONCRETOS AUTO-ADENSÁVEL E CONVENCIONAL COM A MESMA RESISTÊNCIA A COMPRESSÃO

**Ana Lúcia H. de C. El Debs[1] e Fernando M. de Almeida Filho[2]**

Escola de Engenharia de São Carlos – EESC
Universidade de São Paulo – USP
Departamento de Engenharia de Estruturas
CEP: 13566-590 – São Carlos, SP Brasil
[1]E-mail: analucia@sc.usp.br
[2]E-mail: ffilho@sc.usp.br

## ABSTRACT

The present study evaluates the bond behavior between steel bars and self-compacting concrete and ordinary concrete performed in monotonically loaded beam tests, using the Finite Element Method. In the numerical model, concrete and steel bars were represented as non-linear behavior materials, combined with a model of the interaction between steel bars and concrete (contact surface). The aim was to represent the bond phenomena and the beam test result through a numerical approach, comparing these results with International Codes and formulations proposed by the literature. According to the results, the evaluation of the bond behavior for self-compacting concrete and ordinary concrete could be well predicted by some formulations, but several other formulations and the International Codes were conservative giving underestimated test results. The proposed numerical model had a good agreement with the experimental one, especially in the pre-peak branch of the load *vs*. slip and load *vs*. displacement curves. The correct prediction of the bond behavior could lead to reduced development lengths in lap spliced bars and of the steel bar ends in structural elements; besides, the use of self-compacting concrete combined with a reduced development length could lead to an optimized structure with a reduced cost.
**Keywords**: Self-compacting concrete, bond strength, beams, finite element method, steel-concrete interface.

## RESUMO

O presente estudo analisa a representação do comportamento da aderência entre barras de aço e concretos convencionais e auto-adensáveis, realizado em vigas, utilizando o método dos elementos finitos. No modelo numérico, o concreto e a barra de aço foram considerados por comportamento não-linear, combinado com o modelo de interação entre a barra e o concreto adjacente (superfície de contato). O principal objetivo foi representar o fenômeno da aderência do ensaio em vigas através de aproximação numérica, comparando esses resultados experimentais com Códigos Internacionais e formulações propostas na literatura. De acordo com os resultados, a análise do comportamento da aderência tanto para o concreto auto-adensável quanto para o convencional pode ser bem prevista por algumas formulações, mas outras formulações e os Códigos Internacionais foram conservadores fornecendo resultados que subestimaram os resultados experimentais. O modelo numérico proposto obteve uma boa aproximação do resultado experimental, especialmente para o pré-pico do diagrama força *vs*. deslizamento e força *vs*. flecha. A correta previsão do comportamento da aderência pode levar a um menor comprimento de ancoragem em traspasse de barras e em ancoragens de extremidade em elementos estruturais; além disso, a utilização de concreto auto-adensável, combinado com a redução do comprimento de ancoragem poderão conduzir a estruturas otimizadas com redução do seu custo.
**Palavras-Chave**: Concreto auto-adensável, resistência de aderência, vigas, método dos elementos finitos, interface aço-concreto.

## 1 – INTRODUCTION

Self-compacting concrete (SCC) can be defined as a mixture that can be compacted in any place in the formwork, just through the accommodation due to its own weight [1], capable to flow inside of a formwork, flowing by the existing reinforcement and filling it out without the use of any vibration equipments, increasing the productivity and reducing the labor [2].

The bond between steel and concrete is one of the most difficult problems in the study of the concrete and it is still not completely understood. That occurs in function of the high number of theoretical difficulties found to study the bond phenomenon.

The evaluation of the influence of the materials, like self-compacting concrete, and the concern about the rupture of the steel-concrete interface on the bond strength was target of several authors [3-7], showing that the innovative technologies are developed but the Codes and formulations, in general, are very conservative.

The steel-concrete bond is a difficult problem to represent in the study of the reinforced concrete elements and it is not completely understood, because of the great number of variables that are necessary to represent the bond phenomena.

The transfer of forces between the steel bar and adjacent concrete is the fundamental mechanism for the existence of reinforced concrete and this connection is a complex problem that requires many parameters for its correct study.

In the pull-out test of a steel bar from a concrete prism occurs the rupture of the adjacent concrete nearly the deformed bar and the mechanism with pure slip would not be possible [8]. If a steel bar is located close to the concrete prism surface, it will occur the splitting failure of the concrete. On other hand, if no reinforced is added to the concrete prism, the bond resistance depends, almost totally, of the compressive strength of the concrete.

The bond strength varies in function of three parameters, being them: the adhesion; the friction, that is the decisive factor for the bond strength in pieces in the limit state; and the contact interaction among the materials (bearing action), caused by the deformation of the bars in contact with the concrete [9]. Those parameters are influenced strongly by variables as: the mix, temperature and humidity; the age and the values of compressive and tension strength of concrete; deformed bar type and the anchorage length and the speed and type of the load (cyclic or monotonic).

The failure in steel-concrete interface could be attained by combining Coulomb's frictional hypothesis with a bound for the maximum tensile stress (Figure 1), resulting in two different failure modes that could be called sliding failure and separation failure [8]. The sliding failure is assumed to occur in a section when the shear stress exceeds the sliding resistance and should be determined by two parameters: the cohesion (c) and the friction coefficient ($\mu$).

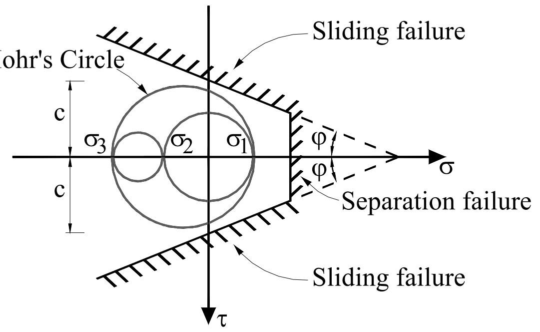


Figure 1. Modified Mohr-Coulomb material [8].

The cohesion will be determined using the Eq.1 and the friction coefficient could be determined by using the Eq. 2 [8].

$$f_c = 2 \cdot c \cdot \sqrt{k} \qquad \text{Eq. 1}$$

$$k = \left(\mu + \sqrt{1+\mu^2}\right)^2 \qquad \text{Eq. 2}$$

In agreement with the literature [8], for low strength concrete and if concrete is identified as a modified Mohr-Coulomb material, the parameter "k" has a value around 4, so, choosing it, the value of $\mu$ will be 0.75, that correspond to a friction angle of $37^o$ and leading to a cohesion equals to 0.75 $kN/cm^2$.

According to the current technical literature, the beam test is more reliable, since its test reflects the influence of the pure flexure and, consequently, the flexural tension cracks. In the literature, there were several beam models used to measure the bond stress, where stand out the Rilem's standard model [10].

The principal aim of this paper is the study of the bond strength of the steel-concrete interface in beam monotonically tested when self-compacting concrete is used. Besides, the evaluation of the effect of the bar size, of 10 and 16 mm, at the failure load was considered. The comparison between several formulations and Codes with the tests performed is made to an evaluation of the bond strength prediction.

The importance of this research lies in the absence of data respects to the behavior of the bond strength between self-compacting concrete with steel bars with different diameters with ordinary concrete with same compressive strength. Also, this research compared self-compacting concrete behavior with the results of several formulations, trying to achieve a better understanding and using this material in civil engineering structures.

## 2 – SUMARY OF EXPERIMENTAL PROGRAM

The experimental program was a part of the research about the bond behavior on self-compacting concrete [11]. In the experimental research, were used two beam specimens based on the model established by Rilem's standards [10], of each series. Figure 2 shows the beam geometry.

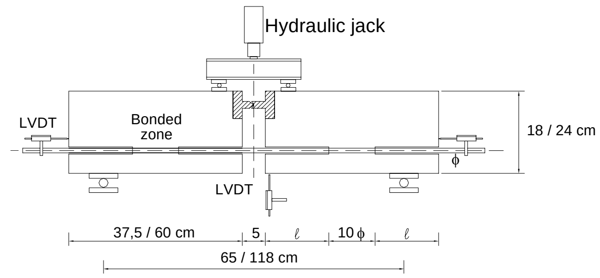


Figure 2. Beam geometry.

The instrumentation, based on LVDT's, was used to measure the bar slip and the vertical displacement, as shown in Figure 2.

According to the literature, specimens cast in the vertical direction present larger bond resistance, while the models with horizontal cast present lower bond strength. In this case, the casting position considered was the second mentioned and a monotonic displacement that changes with the bar diameter was applied. Then, for 10 mm steel bar, the displacement rate was 0.01 mm/s and for the 16 mm steel bar, the displacement rate was 0.016 mm/s, until failure.

The cement used was Ciminas CP-V Ari Plus (Initial High Strength cement). Siliceous sand used had density of 2.63 $kg/dm^3$ and absorption of 4.0% and crushed gravel had density of 2.83 $kg/dm^3$ and absorption of 1.71%. The superplasticizer used was based on carboxylate chains, which density was 1.1 $kg/dm^3$ with 20% of solid content.

Table 1 shows the materials content and the results for SCC and for OC.

Table 1. Materials content and fresh for SCC and for OC.

| Material | OC | SCC | Tests | SCC |
|---|---|---|---|---|
| Cement kg) | 365.3 | 338.8 | Slump test | |
| Sand (kg) | 883.9 | 854.8 | $D_{50}$ (cm) | 67.5 |
| Gravel (kg) | 942.3 | 919.1 | $T_{50}$ (s) | 1.0 |
| Water (kg) | 260.8 | 273.6 | L-Box test | |
| Superpl. (%) | --- | 0.4 | $T_{60}$ (s) | 1.0 |
| Filler (kg) | --- | 101.6 | RB | 0.95 |
| | | | V-Funnel | |
| | | | $T_v$ (s) | 1.5 |

Table 2 shows the hardened properties at the day of the performed test.

Table 2. Hardened properties of SCC and for OC.

| Hardened Properties | OC | SCC |
|---|---|---|
| $f_{c,7}$ (MPa) | 32.02 | 30.10 |
| $E_{c,7}$ (GPa) | 27.24 | 27.87 |
| $f_{ct}$ (MPa) | 2.182 | 2.450 |

According to Table 2, the hardened properties for both concretes were almost the same, which may indicate that the bond strength could present similar behavior.

## 3 – NUMERICAL APPROACH

In previous studies [12-15] the variation of the frictional coefficient and the cohesion seemed not to affect the general response of the bond in the contact surface. However, the number of elements in the contact surface, and parameters like FKN (normal contact stiffness factor), FKT (tangent contact stiffness factor) and IT (iteration number), presented in Ansys® software, affect directly the load *vs.* slip behavior, according to the adopted bond model.

The software used in the numerical simulation was Ansys®, licensed on the Structural Engineering Department of the São Carlos Engineering School, which adopts for the contact formulation the modified Mohr-Coulomb behavior model. A previous study shown that the values of the cohesion and of the frictional coefficient are not important to represent the load *vs.* slip behavior, according to the bonded model criteria adopted [12].

### *3.1 Materials*

For the numerical approach, it was assumed a non-linear behavior of the materials to achieve a better representation of the bond phenomena [12]. The concrete compressive strength and its elasticity modulus were obtained by tests in cylindrical specimens (100 x 200 mm). Figure 3 shows the experimental behavior of SCC and OC and the steel bar behavior assumed in numerical study, and also, the steel bar behavior for 10 and 16 mm bar diameter.

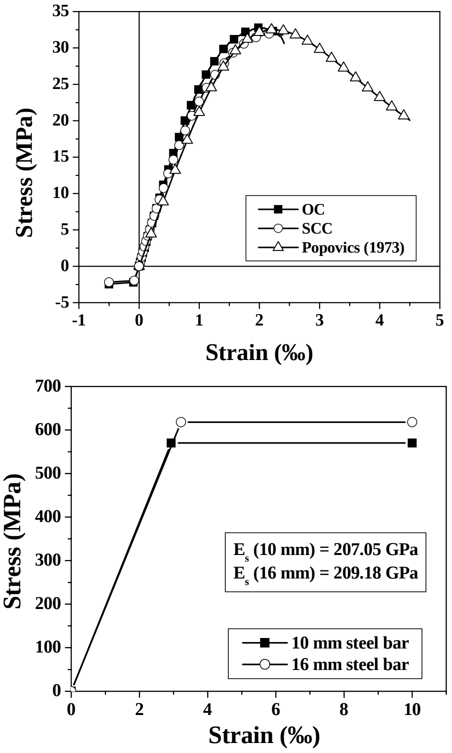


Figure 3. Stress *vs.* strain behavior for steel and for both concretes.

As shown at Figure 3, both concretes behavior were practically the same. However, there was an absence of the descending branch of the post-peak of its behavior, which could be achieved by using Popovics' formulation [16], shown below (Eq. 3 to 5).

$$f_c = f_o \cdot \frac{\varepsilon}{\varepsilon_o} \cdot \frac{n}{n - 1 + \left( \varepsilon / \varepsilon_o \right)^n} \quad \text{Eq. 3}$$

$$n = 0.4 \cdot 10^{-3} \cdot f_o + 1.0 \quad \text{Eq. 4}$$

$$\varepsilon_o = 2{,}7 \cdot 10^{-4} \cdot \sqrt[4]{f_o} \quad \text{Eq. 5}$$

These formulations take into account the variation of the concrete compressive strength in the post-peak branch. According to Popovics' theory, the relation between the initial modulus of elasticity ($E_c$) and the secant modulus of elasticity ($E_{cs}$) can vary until 4.0 for normal strength concretes and in 1.3 for high strength concretes.

### *3.2 Mesh, load and finite elements*

As mentioned before, the geometry of the beam varies according to the bar diameter. The specimen for this study consisted of a steel bar with 10 and 16 mm of nominal diameter, anchored in 100 and 160 mm embedded length in both sides of the concrete beam, respectively.

The roughness of the steel bar was not considered and a plain contact surface was adopted in the numerical study. The finite elements used on the mesh were: for concrete elements, *Solid65*; for steel elements, *Solid45*; for contact surface, *Conta174* and *Targe170* [17].

The load was applied according to the maximum displacement measured on the test at a constant rate. The mesh was made to allow the same point of application of the load as was applied on the test.

Figure 4 shows the mesh used in the numerical models and because of the symmetry; a quarter of the beam model was studied.

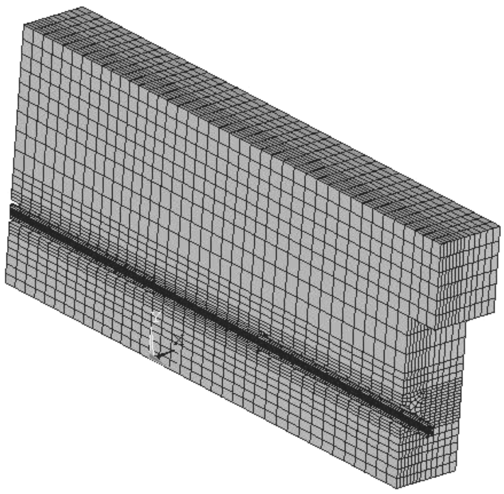

Beam with 10 mm steel bar diameter

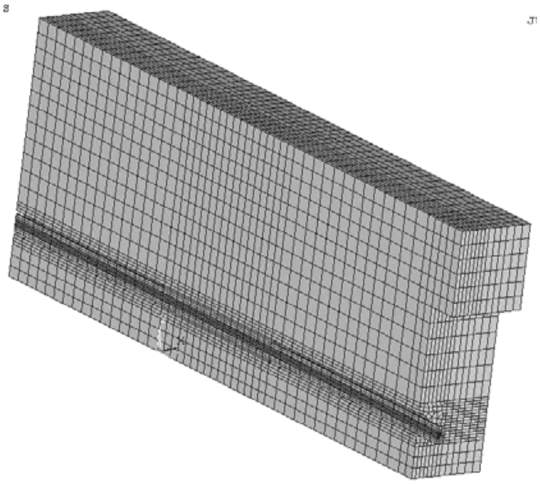

Beam with 16 mm steel bar diameter

Figure 4. Numerical mesh adopted.

### 3.3 Results

The tests results from both concretes were compared with the numerical approach. For each approach was made an analysis of the parameters that possess more influence on its response.

Figure 5 and 6 show the numerical behavior compared with the test results for the beam displacement and its bar slip for 10 and 16 mm steel bar, respectively.

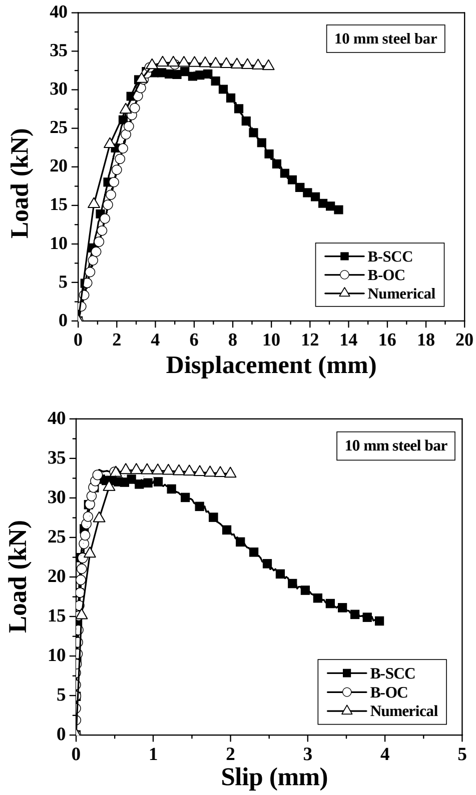


Figure 5. Numerical approaches for 10 mm steel bar.

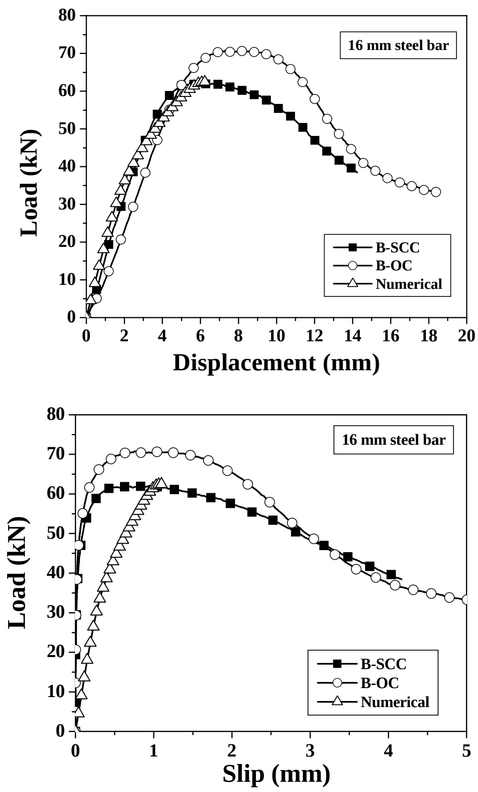


Figure 6. Numerical approaches for 16 mm steel bar.

Table 3 shows the comparison between the numerical and experimental results.

Table 3. Comparison between numerical and test results.

| B-SCC – 10 mm | | | B-OC – 10 mm | |
|---|---|---|---|---|
| | Exp. | Num. /λ | Exp. | Num. /λ |
| $P_u$ (kN) | 32.66 | 32.51/0.97 | 33.49 | 33.51/1.00 |
| $s_u$ (mm) | 0.398 | 0.644/0.62 | 0.295 | 0.644/0.46 |
| $\delta_u$ (mm) | 3.97 | 4.37/0.91 | 3.82 | 4.37/0.87 |

| B-SCC – 16 mm | | | B-OC – 16 mm | |
|---|---|---|---|---|
| | Exp. | Num. /λ | Exp. | Num. / λ |
| $P_u$ (kN) | 61.99 | 62.45/0.99 | 70.77 | 62.45/1.13 |
| $s_u$ (mm) | 0.938 | 1.09/0.85 | 0.758 | 1.09/0.69 |
| $\delta_u$ (mm) | 6.59 | 6.23/1.06 | 7.32 | 6.23/1.18 |

Also, Table 3 shows the used nomenclature for the beams, where “B” referees to beam model, “SCC” and “OC” referees to self-compacting concrete and ordinary concrete, respectively, and “10 mm” and “16 mm” referees to the bar diameter.

According to Table 3, there was a good approach between the numerical and experimental results. The slip of the numerical model was less accurate than the displacement prevision for both steel bar models. The beam model with 10 mm steel bar was better represented by the numerical model than the 16 mm steel bar model. This could be caused by the adopted mesh, which could reduce the accuracy of the numerical approach [12].

Figures 7 and 8 show the principal stresses of the normal direction of the cross section of the beam numerical models of 10 and 16 mm steel bar. Also, the detail of each beam without the steel bar and the steel hinge are shown.

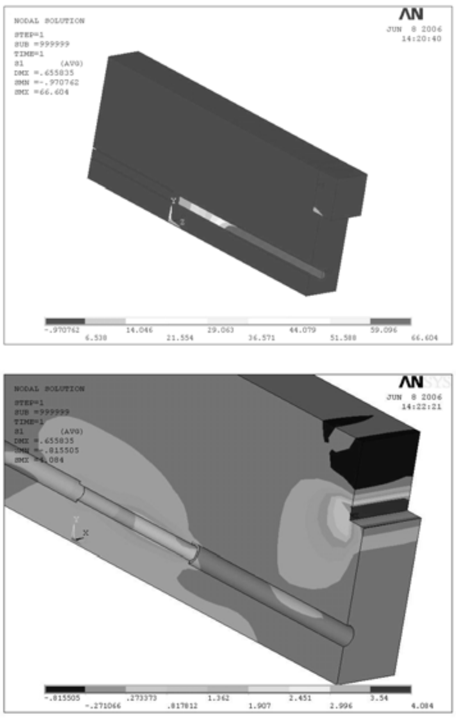

Figure 7. Principal stresses of 10 mm beam models.

According to the numerical results, there is also a variation of the stresses at the steel bar, mainly for the beam with 16 mm steel bar, due to the damage in the model at the beginning of the steel bar. According to the test, due to the high level of vertical displacement, the steel bar increased the stresses near the hinge.

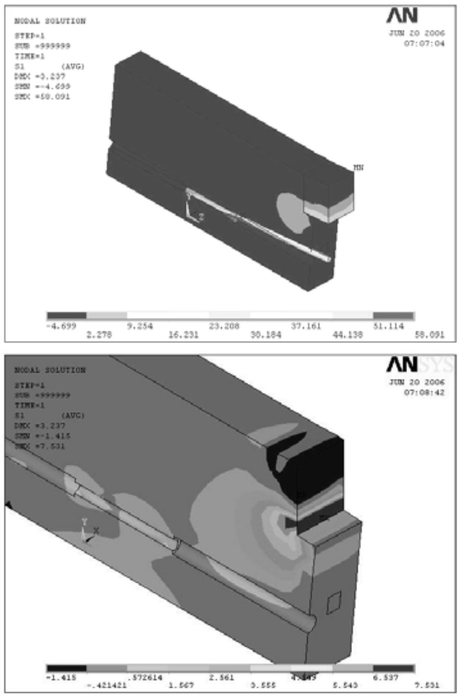

Figure 8. Principal stresses of 16 mm beam models.

The stresses shown in the Figure 7 and 8 are in $kN/cm^2$, and the positive sign indicates tension.

## 4 – COMPARISON WITH THEORETICAL FORMULATIONS

There are several analytic and numerical models in the literature which try to represent the bond stress response in the steel-concrete interface. In those models, most of them were based in experimental data where several parameters were studied like: concrete compressive strength, concrete cover, steel bar diameter, development length and others. The obtained equations allow calculating the average bond strength by means of linear or non-linear regressions from experimental hypothesis. In this paper, the following formulations were used to predict the bond behavior.

$$\tau = \left[1.22 + 3.23 \cdot \left(\frac{c}{\phi_s}\right) + 53 \cdot \left(\frac{\phi_s}{l_d}\right)\right] \cdot \sqrt{f_c} \quad [18] \quad \text{Eq. 6}$$

$$\tau = 232.2 + 2.716 \cdot \frac{c}{\phi_s} \cdot \sqrt{f_c} \quad [19] \quad \text{Eq. 7}$$

$$\tau = \left[3.5 + 3.4 \cdot \left(\frac{c}{\phi_s}\right) + 57 \cdot \left(\frac{\phi_s}{l_d}\right)\right] \cdot \sqrt{f_c} \quad [20] \quad \text{Eq. 8}$$

$$\tau = \left[1.2 + 3 \cdot \left(\frac{c}{\phi_s}\right) + 50 \cdot \left(\frac{\phi_s}{l_d}\right)\right] \cdot \sqrt{f_c} \quad [21] \quad \text{Eq. 9}$$

$$\tau = 19.36 \cdot s^{0,51} \ (f_c < 50 \text{ MPa}) \quad [22] \quad \text{Eq. 10}$$

$$\tau = \left[ 0.324 \cdot \left( \frac{c}{\phi_s} \right) + 5,79 \cdot \left( \frac{\phi_s}{l_d} \right) - 0.879 \right] \cdot \sqrt{f_c} \quad \text{[23] Eq.11}$$

$$\tau = \eta_1 \cdot \eta_2 \cdot \eta_3 \cdot f_{ctd} \quad \text{[24-26] Eq. 12}$$

Those formulations [18-22] were evaluated for conventional concrete with normal and high compressive strength (20-50 MPa). Those expressions were obtained from non-linear regressions with experimental results on different concrete compressive strength.

Table 4 shows the adopted relations for concrete cover – steel bar diameter and steel bar diameter – development length.

Table 4. Established values for theoretical approach

| $\phi_s$ | c | $l_d$ | $c/\phi_s$ | $\phi_s/l_d$ |
|---|---|---|---|---|
| 10 mm | 50 mm | 100 mm | 5 | 0.1 |
| 16 mm | 80 mm | 160 mm | | |

The presented formulations (Eq. 5-11) were obtained from monotonically loaded pull-out tests, which may cause difference among the results. This difference is caused, mainly, by the concrete cover value, which the formulations adopts over five times the bar diameter and by the development length, which for pull-out tests is five times and for beam tests is ten times the steel bar diameter.

The performed beam test used 25 mm of concrete cover, very low in relation to the formulations. The adoption of this value in the equations resulted in low values, and, in one case, below zero [23]. So, the used values for the concrete cover and development length were the same used of the pull-out test (Table 4).

Figure 9 shows the comparison between theoretical and test results.

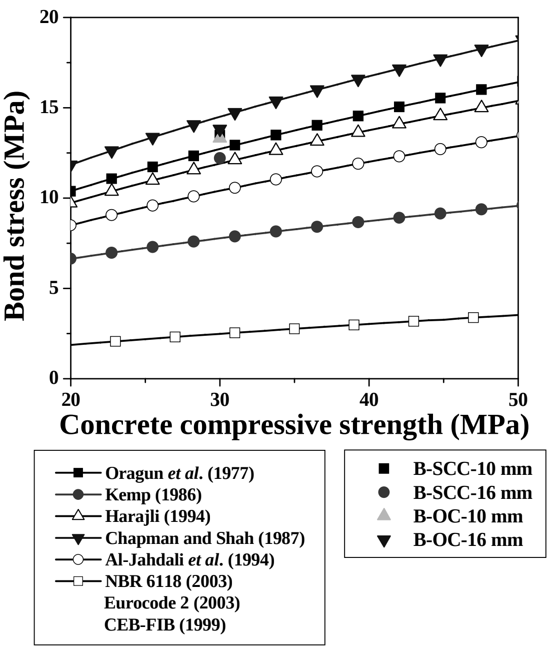


Figure 9. Comparison between theoretical and test results.

According to Figure 9, the values calculated by the theoretical approaches that underestimated the bond strength, exception to the formulation of Chapman & Shah [20]. The best approach was done by Oragun *et al* [18] and Harajli [21]. Also, the Code predictions were very conservative due the assumption of loss of bond when occur the loss of the adhesion, visibly underestimating the bond strength.

Figure 10 shows the ratio between test results and theoretical results for the maximum value for the bond strength for each beam model tested.

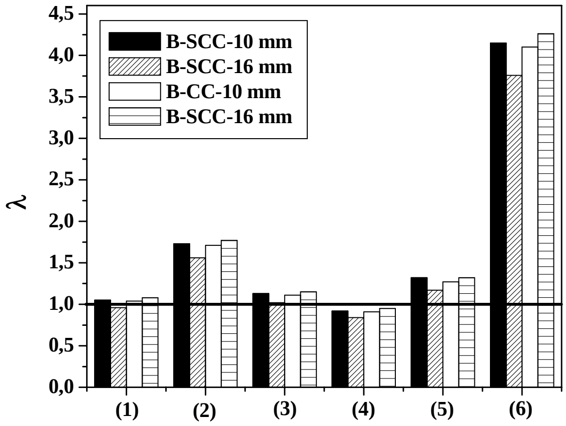


Figure 10. Ratio between tests and theoretical results (λ).

Where, (1) refers to [18]; (2) refers to [19]; (3) refers to [21]; (4) refers to [20]; (5) refers to [23] and (6) refers to [24-26] formulations.

Tables 5 and 6 show the parameters used for the prediction of the bond stress *vs.* slip behavior for the CEB-FIP 195-197 and Huang *et al* [27-28] formulations.

Table 5. Established values for the prediction formulations of Ceb-Fip 195/197 [27], considering good bond conditions.

| | Confined concrete | Non confined concrete |
|---|---|---|
| $s_1$ | 1.0 mm | 0.6 mm |
| $s_2$ | 3.0 mm | 0.6 mm |
| $s_3$ | Distance between ribs | 1.0 mm |
| $\alpha$ | 0.4 | 0.4 |
| $\tau_{máx}$ | $2.5 \cdot \sqrt{f_c}$ | $2.0 \cdot \sqrt{f_c}$ |
| $\tau_u$ | $0.40 \cdot \tau_{máx}$ | $0.15 \cdot \tau_{máx}$ |

Table 6. Established values for the prediction formulations of Huang *et al* [28], considering good bond conditions.

| | High strength concrete | Normal concrete strength |
|---|---|---|
| $s_1$ | 0.5 mm | 1.0 mm |
| $s_2$ | 1.5 mm | 3.0 mm |
| $s_3$ | Distance between ribs | Distance between ribs |
| $\alpha$ | 0.3 | 0.4 |
| $\tau_{máx}$ | $0.40 \cdot f_{cm}$ | $0.40 \cdot f_{cm}$ |
| $\tau_u$ | $0.40 \cdot \tau_{máx}$ | $0.40 \cdot \tau_{máx}$ |

Figure 11 shows the prediction model of the bond stress with the correspondent slip of the steel bar adopted by [27-28].

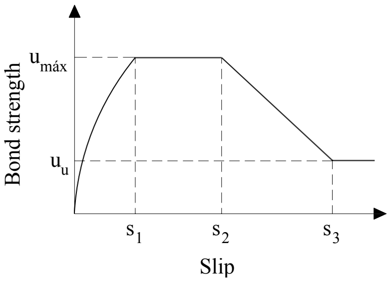


Figure 11. Prediction model for the bond strength [27].

The determination of the bond stress for the correspondent slip is made by the following formulations CEB-FIP 195-197 [27] and Huang *et al* [28].

$$\tau = \tau_{máx} \cdot \left(\frac{s}{s_1}\right)^{\alpha} \qquad \text{For } 0 \le s \le s_1$$

$$\tau = \tau_{máx} \qquad \text{For } s_1 < s \le s_2$$

$$\tau = \tau_{máx} - \left(\tau_{máx} - \tau_u\right) \cdot \left(\frac{s - s_2}{s_3 - s_2}\right) \qquad \text{For } s_2 < s \le s_3$$

$$\tau = \tau_u \qquad \text{For } s_3 < s$$

Figure 12 shows the comparison between the experimental result of the load *vs*. slip behavior with the prediction results of the CEB-FIP 195-197 [27], Huang *et al* [28] and Barbosa [23].

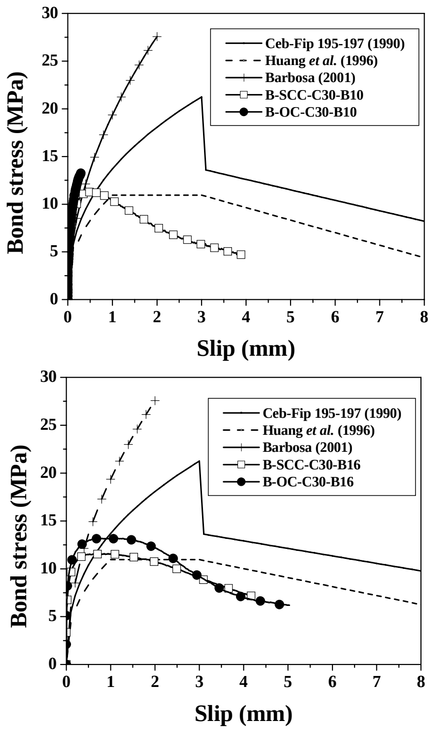


Figure 12. Bond stress-slip behavior comparison between test result and prediction result [22, 27, 28].

According to Figure 11, the mentioned formulations presented a poor approach for both pre-peak and post-peak branch, due to the high values obtained for bond stresses. Only Huang *et al* [28] furnished a better estimation, due to its proximity to the maximum value of the bond stress.

## 4 – CONCLUSIONS

The presented paper describes the numerical approach, based on finite element method, to evaluate the bond stress using beam models based in the Rilem's recommendation, comparing ordinary concrete and self-compacting concrete with the same compressive strength. Also, the test results were compared with theoretical formulations.

According to the results, the following conclusions can be made:

1. The comparison between the beam model with self-compacting concrete and ordinary concrete produced similar results, with a small advantage for the ordinary concrete;

2. The numerical models presented good approach with the tests results, mainly for the failure load and for the displacements value; however, the slip could not be well represented. The difference between the slip compared with the numerical results reached almost 54% (B-OC 10 mm steel bar);

4. The theoretical predictions were very conservative compared to the tests results. Only the formulation of Chapman & Shah (1987) presented values overestimating the test results;

5. The best theoretical approach was reached by Oragun *et al* [18] and Harajli [21];

6. The prediction of the Codes underestimated the bond strength, due to the hypothesis of loss of bond when occur the loss of adhesion;

7. The results from CEB-FIP 195-197 [27], Huang *et al* [28] and Barbosa [22] for the bond stress *vs*. slip showed a poor approach, for both pre-peak and post-peak branch.

Finally, the utilization of numerical models to represent the beam tests, using ordinary concrete and self-compacting concrete, presented good approach. Those values could be extended to models with different compressive strength and bar diameters. The formulations presented good proximity with the test results, mainly Oragun *et al* [18] and Harajli [21]. The approach of the bond stress *vs*. slip behavior was poor denoting the need of a better model.

## LIST OF SYMBOLS

$\tau$ = Bond stress, MPa;
$\tau_u$ = Bond stress at the failure load, MPa;
$P_u$ = Failure load, kN;
$l_d$ = Development length, mm;
$\phi_s$ = Steel bar diameter, mm;
$f_c$ = Concrete compressive strength, MPa;
$s_u$ = Slip at the failure load, mm;
$\delta_u$ = Maximum displacement of the beam, mm;
$\lambda$ = Experimental vs. numerical ratio;

$f_o$ = Cylinder concrete compressive strength, MPa;
$\varepsilon$ = Strain caused by the $f_c$ concrete stress, ‰;
$\varepsilon_o$ = Strain at cylinder concrete failure, ‰.

REFERENCES

[1] Okamura H., "Self-compacting high-performance concrete", Concrete International 19(7):50-54, 1997.
[2] Gomes, P.C.C., "Optimization and characterization of high-strength self-compacting concrete", Doctoral thesis, Universitat Politècnica de Catalunya, 2002.
[3] Dehn, F., Holshemacher, K. and Weiβe, D., "Self-compacting concrete time development of the material properties and the bond behavior", In: LACER, No. 5, 2000.
[4] Holshemacher, K., Dehn, F., Weiβe, D., "Bond in high-strength concrete – influence of rebar position", In: 6th international symposium on utilization of high strength / high-performance concrete, Leipzig-Germany, p.289-298, 2002.
[5] Isa, M.M. and Aguado, A., "Comportamento da aderência entre o concreto auto-adensável de alta resistência e a armadura", In: V Simpósio EPUSP sobre Estruturas de Concreto, São Paulo-Brazil, 2003 (in portuguese).
[6] Almeida Filho, F.M. and El Debs, A.L.H.C., "Pull-out behavior of deformed bars using high strength self-compacting concrete and high strength ordinary concrete", Ibracon Structural Journal, 2(1):44-55, 2006.
[7] Almeida Filho, F.M., De Nardin, S. and El Debs, A.L.H.C., "Evaluation of the bond strength of self-compacting concrete in pull-out tests", In: Second North American Conference on the Design and Use of Self-Consolidating Concrete and Fourth International RILEM Symposium on Self-Compacting Concrete, Chicago October 30 – November 2, 2005.
[8] Nielsen, M.P., "Limit analysis and concrete plasticity", 2nd. Ed., CRC Press, 908 p., ISBN 0-8493-9126-1, 1998.
[9] Bangash, M.Y.H., "Concrete and concrete structures: numerical modeling and applications", Barking: Elsevier science publishers ltd., 687 p., 1989.
[10] Rilem-Fip-Ceb, "Bond test for reinforcing steel: 1-Beam test (7-II-28 D). 2-Pullout test (7-II-128): Tentative recommendations", Materials and Structures, 6(32):96-105, 1973.
[11] Almeida Filho, F.M., "Contribution to study of the bond between steel bars and self-compacting concrete", Doctoral Thesis, Universidade de São Paulo, 2006 (in Portuguese).
[12] Almeida Filho, F.M., De Nardin, S. and El Debs, A.L.H.C., "Interface aço-concreto: análise dos parâmetros do contato e sua influência na simulação via MEF", In: XXV Iberian Latin American Congress on Computational Methods, Recife-PE, Brasil, 2004. (in portuguese)
[13] De Nardin, S., Almeida Filho, F.M., Haach, V.G., Oliveira Filho, J. and El Debs, A.L.H.C., "Non-Linear Analysis of the Bond Strength Behavior on the Steel-Concrete Interface by Numerical Models and Pull-Out Tests", In: ASCE Conference "Structures 2005", Vol. 171, april/2005, New York, USA, 2005, 12 p.
[14] Haach, V.G., Oliveira Filho, J., Almeida Filho, F.M., De Nardin, S. and El Debs, A.L.H.C., "Simulação numérica comparativa do comportamento da aderência em modelos tridimensionais e axissimétricos de arrancamento", In: XXV Iberian Latin American Congress on Computational Methods, Recife-PE, Brasil, 2004.
[15] De Nardin S., Almeida Filho F.M., El Debs, A.L.H.C. and El Debs, M.K., "Steel-concrete interface: influence of contact parameters", In: FIB International Conference: "Keep concrete attractive", May/2005, Budapest, Hungary, 6p, 2005.
[16] Popovics, S., "A numerical approach to the complete stress-strain curves for concrete", Cement and concrete research, 3(5): 583-599, 1973.
[17] Ansys, Manuals on line, 2002.
[18] Oragun, C.O., Jirsa, J.O. and Breen, J.E., "A reevaluation of test data on development length and splices", ACI Journal 74(3):114-122, 1977.
[19] Kemp, E.L., "Bond in reinforced concrete: behavior and design criteria", ACI Journal, 83(1):50-57, 1986.
[20] Chapman, R.A. and Shah, S.P., "Early-age bond strength in reinforced concrete", ACI Materials Journal 84(6):501-510, 1987.
[21] Harajli, M.H., "Development/splice strength of reinforcing bars embedded in plain and fiber reinforced concrete", ACI Structural Journal 91(5):511-520, 1994.
[22] Barbosa, M.T.G., "Evaluation of the behavior of the bond in ordinary and high strength concrete", Doctoral thesis, COPPE/UFRJ, 2001 (in Portuguese).
[23] Al-Jahdali, F.A., Wafa, F.F. and Shihata, S.A., "Development length for straight deformed bars in high-strength concrete", ACI Special Publication (SP-149), p.507-522, 1994.
[24] Brazilian Association of Technical Standards, "NBR 6118: Design of Concrete Structures". Rio de Janeiro, 2003. (in Portuguese).
[25] Ceb-Fip, "Structural Concrete - Bulletin No. 1", Paris, France, 1999.
[26] Eurocode 2, "Design of Concrete Structures - Part 1: General rules and rules for buildings", European Committee of Standardization, Brussels, 2002.
[27] Ceb-Fip, "Comité Euro-International du Béton (Model Code 1990)". Lausane, France, 1990.
[28] Huang, Z., Engström, B. and Magnusson, J. "Experimental investigation of the bond and ancorage behaviour of deformed bars in high strength concrete". Report 94:4, Chalmers University of Technology, 1996.